Research Article

Cancer Immunology Research

PD-1 and LAG-3 Dominate Checkpoint Receptor–Mediated T-cell Inhibition in Renal Cell Carcinoma

Henning Zelba[1], Jens Bedke[2], Jörg Hennenlotter[2], Sven Mostböck[3], Markus Zettl[3], Thomas Zichner[3], Anoop Chandran[1], Arnulf Stenzl[2], Hans-Georg Rammensee[1], and Cécile Gouttefangeas[1]

Abstract

Drugs targeting the programmed cell death protein 1 (PD-1) pathway are approved as therapies for an increasing number of cancer entities, including renal cell carcinoma. Despite a significant increase in overall survival, most treated patients do not show durable clinical responses. A combination of checkpoint inhibitors could provide a promising improvement. The aim of the study was to determine the most promising checkpoint blockade combination for renal cell carcinoma patients. Tumor-infiltrating lymphocytes (TIL) and autologous peripheral blood mononuclear cells (PBMC) were isolated from patients undergoing surgery for primary tumors. Cells were stained for multicolor flow cytometry to determine the (co)expression of five inhibitory receptors (iR), PD-1, LAG-3, Tim-3, BTLA, and CTLA-4, on T-cell populations. The function of these TILs was assessed by intracellular cytokine staining after *in vitro* stimulation in the presence or absence of PD-1 ± LAG-3 or Tim-3–specific antibodies. Although the percentage of iR^+ T cells was low in PBMCs, both $CD4^+$ and $CD8^+$ T cells showed increased frequencies of PD-1^+, LAG-3^+, and Tim-3^+ cells on TILs. The most frequent iR combination was PD-1 and LAG-3 on both $CD4^+$ and $CD8^+$ TILs. Blockade of PD-1 resulted in significant LAG-3, but not Tim-3, upregulation. The dual blockade of PD-1 and LAG-3, but not PD-1 and Tim-3, led to increased IFNγ release upon *in vitro* stimulation. Together, these data suggest that dual blockade of PD-1 and LAG-3 is a promising checkpoint blockade combination for renal cell carcinoma.

Introduction

Renal cell carcinoma (RCC) represents approximately 90% to 95% of all renal tumors in adults (1). Although early-stage RCC has a good prognosis after surgical resection, the mortality rate drastically increases for relapsed or metastatic RCC (mRCC; ref. 2). Treatment options for mRCC have considerably evolved in the last years; on the one hand, targeted therapies (VEGF-tyrosine kinase inhibitors, e.g., sunitinib and mTOR inhibitors, e.g., everolimus) have remarkably improved overall survival (OS), with the approval of several agents for first- or second-line treatment of mRCC (3, 4). On the other hand, RCC tumors are often infiltrated with immune cells and T lymphocytes, an observation that led early on to the notion that the immune system could play an important role in RCC control (5). Hence, immunotherapy has long been considered a relevant treatment option in RCC. Immune targeting treatment has recently shifted from systemic cytokine infusion (IFN-alpha or interleukin-2), to checkpoint inhibitory antibodies that specifically target T cells.

Programmed cell death-1 (PD-1) and cytotoxic T-cell lymphocyte-associated protein 4 (CTLA-4) are major immune-checkpoint molecules that can be successfully targeted by blocking antibodies (Abs) in various tumor entities. Blockade of both PD-1 alone (nivolumab) and in combination with anti–CTLA-4 (nivolumab plus ipilimumab) is clinically approved for advanced RCC by the FDA (6). Second- or third-line treatment with nivolumab alone improves clinical response (objective response rate, ORR) and prolongs OS as compared with everolimus (ORR: 25 versus 5%; median OS: 25 vs. 20 months for the Ab therapy versus mTOR inhibition, respectively; ref. 7). Data from a late phase III trial (Checkmate 214) demonstrate that nivolumab in combination with ipilimumab is superior to sunitinib in previously untreated patients (ORR: 42 vs. 27%; median OS: not reached versus 26 months; ref. 8).

Despite impressive objective response rates and indubitable survival benefit for RCC and many other tumor types, checkpoint blockade with CTLA-4 and/or PD-1 antibodies is not effective in a large fraction of treated patients (9). Predictive biomarkers are therefore being intensively studied at the moment. The expression of PD-L1 (the ligand of PD-1) within the tumor, the extensive tumor infiltration by $CD8^+$ tumor-infiltrating lymphocytes (TIL), and high tumor mutational burden are the most accurate and specific biomarkers of clinical response to checkpoint blockade (10–13). Furthermore, expression of additional inhibitory

[1]Department of Immunology, University of Tübingen, Tübingen, Germany. [2]Department of Urology, University Hospital Tübingen, Tübingen, Germany. [3]Boehringer Ingelheim RCV GmbH & Co KG, Vienna, Austria.

Note: Supplementary data for this article are available at Cancer Immunology Research Online (http://cancerimmunolres.aacrjournals.org/).

Current address for H. Zelba: CeGaT GmbH, Tübingen, Germany; and current address for M. Zettl: Pieris Pharmaceuticals, Inc., Munich, Germany.

Corresponding Authors: Henning Zelba, Department of Immunology, University of Tübingen, Auf der Morgenstelle 15, 72076 Tübingen, Germany. Phone: 49-7071-29-80994; Fax: 49-7071-29-5653; E-mail: henning_zelba@gmx.de; and Cécile Gouttefangeas, Department of Immunology, University of Tübingen, Auf der Morgenstelle 15, 72076 Tübingen, Germany. Phone: 49-7071-29-80994; Fax: 49-7071-29-5653; E-mail: cecile.gouttefangeas@uni-tuebingen.de

Cancer Immunol Res 2019;7:1891–9

doi: 10.1158/2326-6066.CIR-19-0146

receptors (iR) by intratumoral effector T cells, such as Tim-3, LAG-3, or TIGIT, or even downregulation of activating checkpoint receptors (e.g., CD28, OX-40, CD27) might explain, at least partially, resistance to PD-1 and/or CTLA-4 blockade (14, 15). In primary clear cell RCC (ccRCC), PD-1 and LAG-3 expression within the tumor inversely correlates with patient disease-free and OS. For example, patients with high density of LAG-3$^+$ cells in the invasive margin but not the tumor center displayed a shorter disease-free survival and a tendency toward reduced OS (16). Furthermore, coexpression of Tim-3 and PD-1 iR has been associated with greater T-cell exhaustion and poorer clinical outcome (17).

Thus, for RCC and other tumors, the combination of checkpoint inhibitors is currently one the most promising treatment approaches. In order to identify which receptors to target and the most promising combination of antibodies that could induce robust clinical outcomes, a precise knowledge of the receptor expression and coexpression on immune cells in general, and on tumor-infiltrating T-cell subsets, is essential. In this study, we assessed the coexpression of several inhibitory checkpoint receptors in advanced RCC. Our overall objective was to identify the most promising blocking antibody combination(s) for clinical application. PBMCs and autologous TILs were collected from 35 patients who did not receive checkpoint therapy prior to surgery; the expression and coexpression patterns of five common inhibitory receptors (PD-1, Tim-3, LAG-3, BTLA, and CTLA-4) were assessed followed by *in vitro* checkpoint blockade using a combination of blocking antibodies specific for the most expressed receptors. Our data show that blocking PD-1 and LAG-3 together is a promising strategy in RCC.

Table 1. Patient characteristics

Parameter	Classification	Number	%	Patients with relapse
Total		35	100	6
Median age		73 years		
Gender	Male	25	71	4
	Female	10	29	2
RCC subtype	Clear cell	29	83	5
	Chromophobe	4	11	0
	Clear cell + sarcomatoid	2	6	1
T stage	1	22	63	2
	2	4	11	0
	3	8	23	3
	4	1	3	1
G stage	1	8	23	0
	2	20	57	4
	3	6	17	2
	n.a.	1	3	–
N stage	0	31	88	5
	1	2	6	1
	n.a.	2	6	–
M stage	0	26	74	2
	1	7	20	4
	n.a.	2	6	–
Median tumor diameter		5.5 cm		
Median amount of TILs/g		5.7×10^6 cells		

Abbreviation: n.a., not available.

Materials and Methods

Patients

Thirty-five patients with clear cell or chromophobe RCC at any stage of disease were enrolled in the study. None of these patients had received checkpoint therapy before enrollment. The inclusion criteria were as follows: age > 18 and Eastern Cooperative Oncology Group (ECOG) performance status 0 to 1. The exclusion criteria were as follows: cachexia or anemia (hemoglobin< 10 g/100 mL). Tumor type, stage, and clinical course are given in Table 1, and details for individual patients are listed in Supplementary Table S1. Recruitment started in 2013 and lasted for 26 months. Cutoff for clinical follow-up was 6 months after recruitment of the last patient. The study was conducted in accordance with the Declaration of Helsinki and was approved by the Ethics Committee of the University Hospital of Tübingen (Ethik-Kommission an der Medizinischen Fakultät der Eberhard-Karls-Universität und am Universitätsklinikum Tübingen; approval number 555/2013BO2) and patients were included after signed informed consent.

Cell isolation and preparation

Fresh tumor tissue and autologous blood were collected at surgery. Blood was drawn in Li-Hep monovettes (Sarstedt) and peripheral blood mononuclear cells (PBMC) isolated using standard density centrifugation with Ficoll/hypaque (Biochrom GmbH), washed in sterile PBS, counted with trypan blue, then cell aliquots were frozen in liquid nitrogen (−196°C). Briefly, cells resuspended in FCS + 10% DMSO and kept in a freezing container (Mr. Frosty; Thermo Fisher Scientific) were immediately transferred to a −80°C freezer. After at least 24 hours, frozen cells were transferred into a liquid nitrogen tank (18). PBMCs from healthy donors (HD) were isolated from buffy coats obtained from the local blood bank following the same procedure, and also frozen until use.

For isolation of TILs, fresh primary renal tumor tissue was dissociated into single-cell suspension by a combined mechanical and enzymatic procedure using the gentleMACS Dissociator and the Tumor Dissociation Kit, human (both Miltenyi Biotec), essentially as per manufacturer's instructions. Briefly, fresh tumor tissue was cut into pieces of 1–8 mm^3 and transferred into C Tubes (Miltenyi Biotec) containing a mix of enzymes H and A. Two mechanical dissociation steps with the gentleMACS Dissociator (programs h_tumor_01 + h_tumor_02, then h_tumor_03) were applied, each followed by incubation for 30 minutes at 37°C under agitation. After washing with PBS, cells were filtered through a 100-μm cell strainer (BD Biosciences), counted with trypan blue, and stored in liquid nitrogen. Cryopreserved samples were stored between 1 and 11 months until usage.

Phenotype analysis

Phenotypic analysis was performed as previously described (19). Briefly, a preestablished panel with all antibodies being used at optimal pretested concentrations, was used for the phenotyping of TILs and autologous PBMCs. Cryopreserved cells (TILs and PBMCs) were thawed and 0.5×10^6 cells were washed with staining buffer (PBS, 2% heat-inactivated FCS, 2 mmol/L EDTA, 0.02% sodium azide) and stained for extracellular surface markers with the following monoclonal antibodies (mAb): CD3-PE-Cy5.5 (clone SK7; eBioscience), CD4-BV711 (clone OKT4; BioLegend), CD8-PerCP (clone SK1; BioLegend), BTLA-PE (clone MIH26; BioLegend), PD-1-APC-Cy7 (clone EH12.2H7; BioLegend), LAG-3-ATTO647 (clone 17B4; Enzo Life Sciences), Tim-3-PE-Cy7 (clone F38-2E2;

BioLegend), CTLA-4-PE-CF594 (clone BNI3; BD Biosciences), CD39-BV421 (clone A1; BioLegend), CD25-BV605 (clone BC96; BioLegend), CD45RA-BV570 (clone HI100; BioLegend), CCR7-BV650 (clone G043H7; BioLegend), or corresponding isotype controls from the same manufacturers. Dead cells were stained using Aqua Live/Dead dye (Thermo Fisher Scientific) added during Ab incubation. After extracellular staining, cells were washed, fixed, and permeabilized using a fixation/permeabilization solution (eBioscience) according to the manufacturer's instructions, followed by intracellular staining using Foxp3-FITC (clone PCH101; eBioscience) and Ki67-AlexaFluor 700 (clone B56; BD Biosciences) or corresponding isotype controls, followed by two final wash steps. The full Ab panel is shown in Supplementary Table S2.

In vitro checkpoint blockade

Based on preliminary experiments, TIL functionality was assessed by intracellular cytokine staining after 3 days of *in vitro* stimulation. Briefly, 0.5×10^6 cells were seeded in a 24-well plate in IMDM (Lonza) containing glutamine, 0.5% penicillin/streptomycin and heat-inactivated human AB serum (all Sigma-Aldrich) and stimulated with precoated CD3 Ab (clone OKT3 at 0.25 μg/mL, eBioscience) in the presence of one or two added antagonistic mAbs at 10 μg/mL (anti–PD-1, anti–LAG-3, and anti–Tim-3) or corresponding isotype control antibodies. This concentration induces maximum effects *in vitro* (20–22) and is also compatible with the reported *in vivo* pharmacokinetics of PD-1–specific antibodies (23, 24). Blocking with anti–PD-1 alone was performed for all patients tested ($n = 25$). Due to the limited number of TILs for some patients, dual blocking with anti–PD-1 plus anti–LAG-3 was performed for $n = 19$ patients (preferred combination) and with anti–PD-1 plus anti–Tim-3 for $n = 7$ patients. After 72 hours of incubation, a CD107a-FITC antibody (clone H4A3; BD Biosciences) and Golgi inhibitors (GolgiStop 1:1,500, BD Biosciences, and 10 μg/mL Brefeldin-A, Sigma-Aldrich) were added, and cells were further incubated for 12 hours.

To assess checkpoint receptor expression after antagonist Ab treatment, cells were stained with Abs CD4-BV711 (clone OKT4; BioLegend), CD8-PerCP (clone SK1; BioLegend), Tim-3-PE-Cy7 (clone F38-2E2; BioLegend), LAG-3-ATTO647 (clone 17B4; Enzo), an anti-human IgG4-PE (Southern Biotec) against the PD-1 blocking Ab, and with Aqua Live/Dead (Thermo Fisher Scientific). The functional Ab panel is shown in Supplementary Table S2. After fixation and permeabilization using a fixation/permeabilization solution (BD Biosciences), cells were intracellularly stained with Ki67-AlexaFluor 700 (clone B56; BD Biosciences) and IFNγ-BV421 (clone 4S.B3; BioLegend) Ab, washed twice and resuspended in FACS buffer.

Data acquisition and analysis

All samples were acquired on an LSRFortessa SORP cytometer (BD Biosciences) operated through the BD FACSDivaTM software (Version 6.1.2). Spectral overlap was compensated using AbC and ArC beads (both Life Technologies). The resulting data were saved as FCS 3.0 files and subsequently analyzed using FlowJo (Windows version V10; FlowJo LLC). Samples were serially gated following established gating strategies (see Supplementary Fig. S1). Within single, viable lymphocytes, we gated on $CD3^+$ and $CD3^-$ cells. $CD3^+$ cells were further discriminated into $CD4^+CD8^-$ (total $CD4^+$ T cells), $CD4^-CD8^+$ ($CD8^+$ T cells), and $CD4^-CD8^-$ (DN) T cells. Within total $CD4^+$ T cells, $CD25^+Foxp3^+$ were defined as being regulatory T cells (Treg), whereas all remaining $CD4^+$ T cells, i.e., non-Tregs, were defined as conventional $CD4^+$ T cells (hereinafter referred to as T_{conv}). Gates were placed according to isotype control stainings. Only samples with at least $n = 1{,}000$ total $CD4^+$ and/or $CD8^+$ T cells were included in this study. Boolean gating, using the operators "AND," "OR," and "NOT," was applied to analyze checkpoint receptor coexpression on T-cell subsets. All experiments were performed and analyzed centrally by one investigator. Normally distributed values were compared using a Student t test. Nonparametric values were compared using the Mann–Whitney test. All statistical analyses were performed using GraphPad Prism 5 (GraphPad Software Inc.) and SPSS Statistics 24 (IBM).

Multivariate analysis

Cluster analysis and heat-map visualization was performed based on the iR^+ cell frequencies using R 3.5.0 (R Core Team (2018)/R: A language and environment for statistical computing. R Foundation for Statistical Computing, Vienna, Austria, https://www.R-project.org/), and the R package pheatmap 1.0.10 (Raivo Kolde (2018)/pheatmap: Pretty Heatmaps, R package version 1.0.10, https://CRAN.R-project.org/package=pheatmap), using default parameters. The clustering was determined based on hierarchical clustering using eucledian distance and the "complete" method.

Results

Patient characteristics

Thirty-five RCC patients undergoing surgical removal of primary kidney tumors were included in the study. The median age of patients was 73 years, with an interquartile range (IQR) of 54 to 78 years. Seventy-one percent of the patients were male. Tumors were confirmed by pathologic examination as being clear cell ($n = 29$), chromophobe ($n = 4$), and clear cell/sarcomatoid ($n = 2$) carcinomas; papillary RCC were not included. Sixty-three percent

Table 2. iR coexpression on effector RCC $CD4^+$ and $CD8^+$ TILs

Combination	Number of iR expressed	Mean % within $CD4^+$ T_{conv}	SD	Combination	Number of iR expressed	Mean % within $CD8^+$	SD
$BTLA^-$ $CTLA\text{-}4^-$ $LAG\text{-}3^-$ $PD\text{-}1^-$ $Tim\text{-}3^-$	0	26.17	±16.72	$BTLA^-$ $CTLA\text{-}4^-$ $LAG\text{-}3^-$ $PD\text{-}1^-$ $Tim\text{-}3^-$	0	23.64	±16.98
$BTLA^+$ $CTLA\text{-}4^-$ $LAG\text{-}3^-$ $PD\text{-}1^-$ $Tim\text{-}3^-$	1	18.30	±17.37	$BTLA^-$ $CTLA\text{-}4^-$ $LAG\text{-}3^-$ $PD\text{-}1^+$ $Tim\text{-}3^-$	1	16.82	±13.84
$BTLA^-$ $CTLA\text{-}4^-$ $LAG\text{-}3^-$ $PD\text{-}1^+$ $Tim\text{-}3^-$	1	13.54	±11.97	$BTLA^-$ $CTLA\text{-}4^-$ $LAG\text{-}3^+$ $PD\text{-}1^+$ $Tim\text{-}3^-$	2	10.11	±13.08
$BTLA^-$ $CTLA\text{-}4^-$ $LAG\text{-}3^+$ $PD\text{-}1^+$ $Tim\text{-}3^-$	2	8.81	±11.71	$BTLA^-$ $CTLA\text{-}4^-$ $LAG\text{-}3^+$ $PD\text{-}1^+$ $Tim\text{-}3^+$	3	9.33	±14.51
$BTLA^-$ $CTLA\text{-}4^-$ $LAG\text{-}3^+$ $PD\text{-}1^-$ $Tim\text{-}3^-$	1	7.38	±9.98	$BTLA^-$ $CTLA\text{-}4^-$ $LAG\text{-}3^+$ $PD\text{-}1^-$ $Tim\text{-}3^-$	1	9.09	±15.95
$BTLA^+$ $CTLA\text{-}4^-$ $LAG\text{-}3^+$ $PD\text{-}1^-$ $Tim\text{-}3^-$	2	5.70	±10.37	$BTLA^+$ $CTLA\text{-}4^-$ $LAG\text{-}3^-$ $PD\text{-}1^-$ $Tim\text{-}3^-$	1	6.97	±9.91
$BTLA^+$ $CTLA\text{-}4^-$ $LAG\text{-}3^-$ $PD\text{-}1^+$ $Tim\text{-}3^-$	2	4.68	±5.19	$BTLA^-$ $CTLA\text{-}4^-$ $LAG\text{-}3^-$ $PD\text{-}1^+$ $Tim\text{-}3^+$	2	6.38	±9.20

NOTE: Top seven most frequent iR combinations (by mean frequencies from $n = 35$ RCC patients) for $CD4^+$ T_{conv} (left) and $CD8^+$ T cells (right) in TILs.

of the tumors were assigned to the T1 category, 11% to the T2, 23% to the T3, and 3% to the T4 category. Seven patients had metastases at the time of surgery; this information was missing for 2 patients. Lactate dehydrogenase (LDH) level, a surrogate marker for cancer progression which is routinely determined at the University Hospital Tübingen, was known for $n = 32$ patients. Median LDH was 210 U/L (IQR 121–250). Clinical follow-up was available for $n = 33$ patients (median follow-up time = 13 months, IQR 5–19 months); during this time, $n = 6$ patients relapsed with a median time to progression of 3.5 months (IQR 3–9). Patient characteristics are shown in Table 1 and in Supplementary Table S1. PBMCs from $n = 15$ HD were included as control samples. Median age was 56 years, with an IQR of 43 to 64 years. Seventy-three percent of the HD were male.

PD-1 and LAG-3 were the most frequently upregulated iR within RCC TILs

The expression of five common iR, i.e., PD-1, LAG-3, Tim-3, BTLA, and CTLA-4, was assessed on $CD8^+$ and on non-Treg $CD4^+$ cells ($CD4^+$ T_{conv}) in TILs and autologous PBMCs. As a comparison, iR expression was also evaluated on $CD8^+$ T cells and $CD4^+$ T_{conv} in PBMCs from healthy blood bank donors (HD_PBMCs). Within TILs, PD-1 (median percentage of PD-1^+ cells within $CD4^+$ T_{conv}: 35.3%; within $CD8^+$ T cells: 59.6%), followed by LAG-3 (T_{conv}: 25.0%; $CD8^+$: 27.3%) and BTLA ($CD4^+$ T_{conv}: 35.5%; $CD8^+$: 18.1%) were the most frequently expressed inhibitory receptors, whereas Tim-3 and CTLA-4 were expressed on a smaller fraction of cells (median $CD4^+$ T_{conv}: 4.3% and 2.5%; $CD8^+$: 16.4% and 3.2% for each marker, respectively; Fig. 1). The median frequencies of PD-1^+, LAG-3^+, Tim-3^+, and CTLA-4^+ (only on $CD4^+$ T_{conv}) T cells were significantly increased in TILs compared with autologous blood T cells; in particular, PD-1 was increased by at least 2-fold in TILs versus PBMCs in more than 69% of the patients. Interestingly, the expression of LAG-3 on $CD8^+$ T cells appeared to define two groups of patients with moderate (< 40% of the cells; median percentage within $CD8^+$: 12.4%) or high (> 60% of the cells; median percentage $CD8^+$: 77.4%) expression. Only the percentage of $BTLA^+$ cells was decreased in TILs versus PBMCs (Fig. 1).

In RCC_PBMCs, only the percentage of PD-1^+ was significantly increased in both $CD4^+$ T_{conv} and $CD8^+$ cells as compared with PBMCs of HD (median $CD4^+$ T_{conv}: 10.5% vs. 5.3%; $CD8^+$: 19.2% vs. 9.0%). The frequency of $BTLA^+$ $CD4^+$ T_{conv} was also considerably increased in RCC patients (81.2% vs. 34.4%). Overall, the expression of Tim-3, LAG-3, and CTLA-4 was only marginal (< 5%) in blood T cells (Fig. 1).

The percentage of Tregs (defined as being $CD3^+$, $CD4^+$, $CD25^+$, and $Foxp3^+$) was increased in TILs (median 9.7%; IQR range 6.4%–15.3%) compared with autologous PBMCs (median 3.5%; range, 2.4%–4.9%), in accordance with our previous observation (25). However, it was significantly decreased within RCC_PBMCs compared with HD_PBMCs (median 5.0%; range, 4.2%–6.4%). Interestingly, the expression profile of the five iR on tumor-infiltrating Tregs was different from that of effector T cells, because four receptors (PD-1, LAG-3, Tim-3, and CTLA-4) were significantly upregulated, whereas the percentage of $BTLA^+$ Tregs was not altered (Supplementary Fig. S2).

Altogether, the increased expression of PD-1, LAG-3, and to a lesser extent Tim-3 was observed on all subsets of tumor-infiltrating T cells, whereas CTLA-4 was preferentially upregulated on Tregs, and BTLA downregulated on $CD8^+$ and $CD4^+$ T_{conv}. Notably, the vast majority, i.e., 87.4% (range, 50.5%–98.5%) of $CD4^+$ T_{conv} and 80.0% (range, 40.1%–94.6%) of $CD8^+$ TILs showed an effector memory (EM) phenotype ($CD45RA^-$ $CCR7^-$; EM RCC_PBMCs: 27.9% within $CD4^+$ T_{conv} and 40.0% within $CD8^+$ T cells), as shown in Supplementary Fig. S3. These results are in accordance with our previous observation (25).

Correlation analysis identified two main patient groups

In order to integrate phenotypic and clinical parameters that were gained from our analyses of tumor-infiltrating cells, we performed an unsupervised clustering analysis based on the iR^+ cell frequencies (Fig. 2). This identified two main subgroups of patients (groups 1 and 2), whereby group 1 was dominantly characterized by no expression of LAG-3 and group 2 by coordinated and frequent expression of LAG-3: when LAG-3 expression was prominent, we could mostly detect high frequencies of LAG-3^+ cells in all cell compartments [non-lymphocytes, Tregs, $CD4^+$

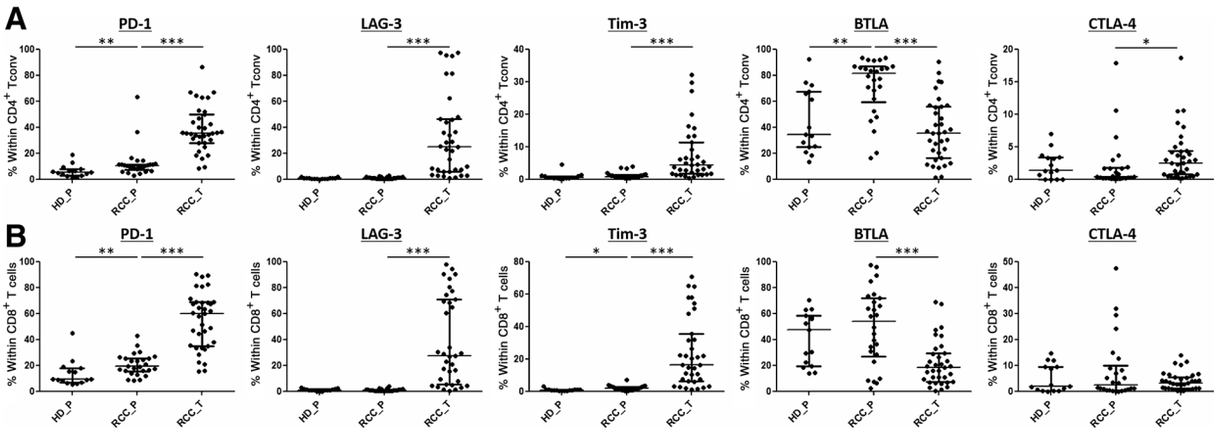

Figure 1.

Checkpoint receptor expression in T cells from RCC patients. Frequency of iR^+ cells within $CD4^+$ T_{conv} (**A**) and $CD8^+$ T cells (**B**) in TILs (RCC_T; $n = 35$), autologous PBMCs (RCC_P; $n = 35$), and HD PBMCs (HD_P; $n = 15$). Median and IQR are shown. Asterisks indicate results from *t* test (paired between RCC_P and RCC_T and unpaired between RCC_P and HD_P. LAG-3 was not normally distributed and was tested with a Mann–Whitney test; *, $P \leq 0.05$; **, $P \leq 0.01$; ***, $P \leq 0.001$).

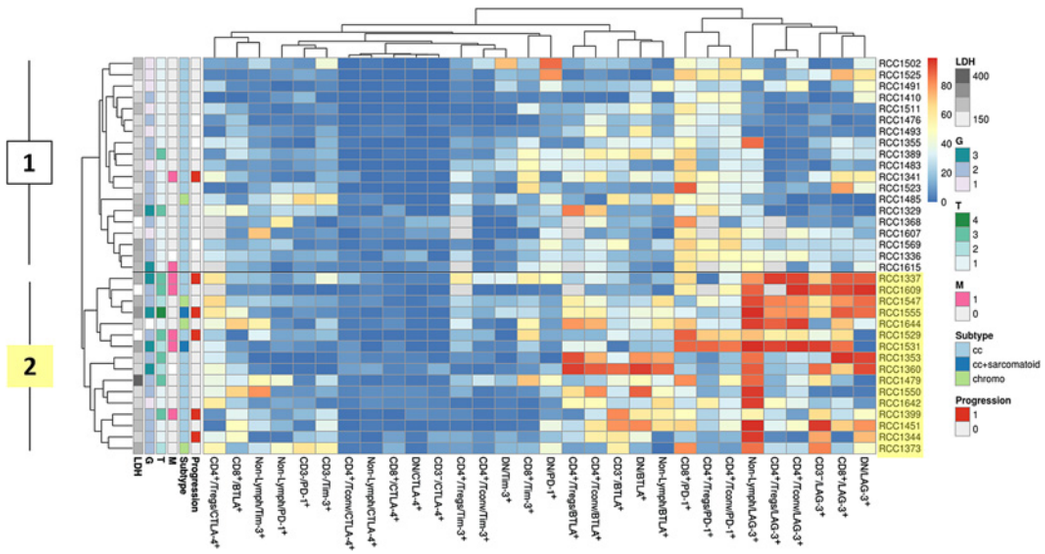

Figure 2.

Heat map showing the frequencies of immune populations within tumors. Hierarchical clustering of patients was performed according to indicated frequencies of iR^+ immune populations as determined by flow cytometry analysis (color gradient from dark blue = 0% to dark red = 100% of the parent cell subset). Definition of main cell subsets was performed according to the gating strategy shown in Supplementary Fig. S1. Clinical parameters depicted on the right (LDH, G-, T-, and M-stage, subtype, and progression) were not included in the clustering. Clustering resulted in two patient groups (1 and 2). chromo, chromophobe; DN, $CD4^-CD8^-$ T cells.

T_{conv}, $CD8^+$ T cells but also $CD3^-$, and $CD3^+$ $CD4^-$ $CD8^-$(DN) lymphocytes; Fig. 2].

Patients from group 2 showed significantly higher LDH serum concentrations compared with patients from group 1 (mean 244.1 vs. 193.3 U/L; $P = 0.0158$ Mann–Whitney test; Fig. 2). Baseline levels of LDH are associated with survival upon checkpoint blockade therapy (26). T stage was more advanced in patient group 2 (44% vs. 11% of patients had T3 or T4 in group 2 and group 1, respectively; $P = 0.0498$, Fisher exact test), whereas M stage (31% vs. 11% of patients were M1; $P = 0.2075$, Fisher exact test) and progression rate (31% vs. 5% of patients relapsed; $P = 0.0728$, Fisher exact test) were not different between the two groups (Fig. 2). Hence, LAG-3 (but not PD-1 or Tim-3) expression in various tumor-infiltrating immune cells defines two subgroups of RCC patients, and, in accordance with previous observations (16, 27), might be associated with tumor progression and parameters of comparatively bad clinical course.

PD-1 and LAG-3 were the most frequently coexpressed iR within RCC TILs

The use of multicolor flow cytometry allowed us to investigate the coexpression of the five iR at a single-cell level within the TIL populations. Boolean analysis of 5 parameters on the two effector T-cell subsets, i.e., $CD8^+$ and $CD4^+$ T_{conv}, resulted in 32 different populations, each with a distinct iR expression profile; mean expression and SD were calculated. Table 2 shows the 7 most frequent combinations for $n = 35$ patients: interestingly, we found that approximately one fourth of both $CD4^+$ T_{conv} and $CD8^+$ T cells did not express any of the five tested iR (mean 26.2% and 23.6%, respectively), and that this population was the most represented within TILs. Cells expressing only PD-1 or only LAG-3 but none of the other four iR were also frequently observed (13.5% and 7.4% of the $CD4^+$ T_{conv} subset; 16.8% and 9.1% of the $CD8^+$ T cells for PD-1 and LAG-3, respectively; Table 2). The most frequent iR combination was PD-1 and LAG-3 without BTLA, CTLA-4, and Tim-3 ($CD4^+$ T_{conv}: 8.8%; $CD8^+$ T cells: 10.1%; Table 2). Cells expressing only PD-1 plus Tim-3 were less frequent ($CD4^+$ T_{conv}: 1.3%; $CD8^+$ T cells: 6.4%), while specifically in the $CD8^+$ T-cell subset, > 9% of the cells expressed the three iR PD-1, LAG-3 and Tim-3 simultaneously (Table 2). Other combinations, especially cells bearing more than two iR, were rare and accounted for less than 5% of the total cells (Table 2). The mean frequency of each of the 32 populations is listed in Supplementary Table S3.

Finally, when considering $PD\text{-}1^+$ cells, which was the most frequent subpopulation in single iR analysis (Fig. 1), LAG-3 was coexpressed in approximately half of the cells (46.0% and 47.7% of $CD4^+$ T_{conv} $PD\text{-}1^+$ and $CD8^+$ $PD\text{-}1^+$, respectively), and Tim-3 on approximately 40% of the $CD8^+$ $PD\text{-}1^+$ and only 16% of the $CD4^+$ T_{conv} $PD\text{-}1^+$. BTLA and CTLA-4 were only marginally present on $PD\text{-}1^+$ cells (less than 15% of the $CD4^+$ or $CD8^+$ cells for BTLA and less than 5% of the same subsets for CTLA-4). Altogether, the majority (between 50% and 65%) of the $CD4^+$ and $CD8^+$ potential TIL effectors did express either PD-1 and/or LAG-3, often together with Tim-3, whereas approximately one fourth did not express any of the five iR tested (Table 2).

Dual PD-1 and LAG-3 blockade improved T-cell function *in vitro*

To investigate the functional impact of iR coexpression, we established a short-term culture system whereby TILs were cultured for 3 days in the presence of a CD3 antibody either together with one or more blocking anti-iR, or without checkpoint blockade (relevant isotype control antibodies) as a control. Because PD-1, followed by LAG-3 and Tim-3 was the most frequently upregulated iR in the RCC TILs, we used anti–PD-1 alone or together with either anti–LAG-3 or anti–Tim-3. Following this *in vitro* stimulation

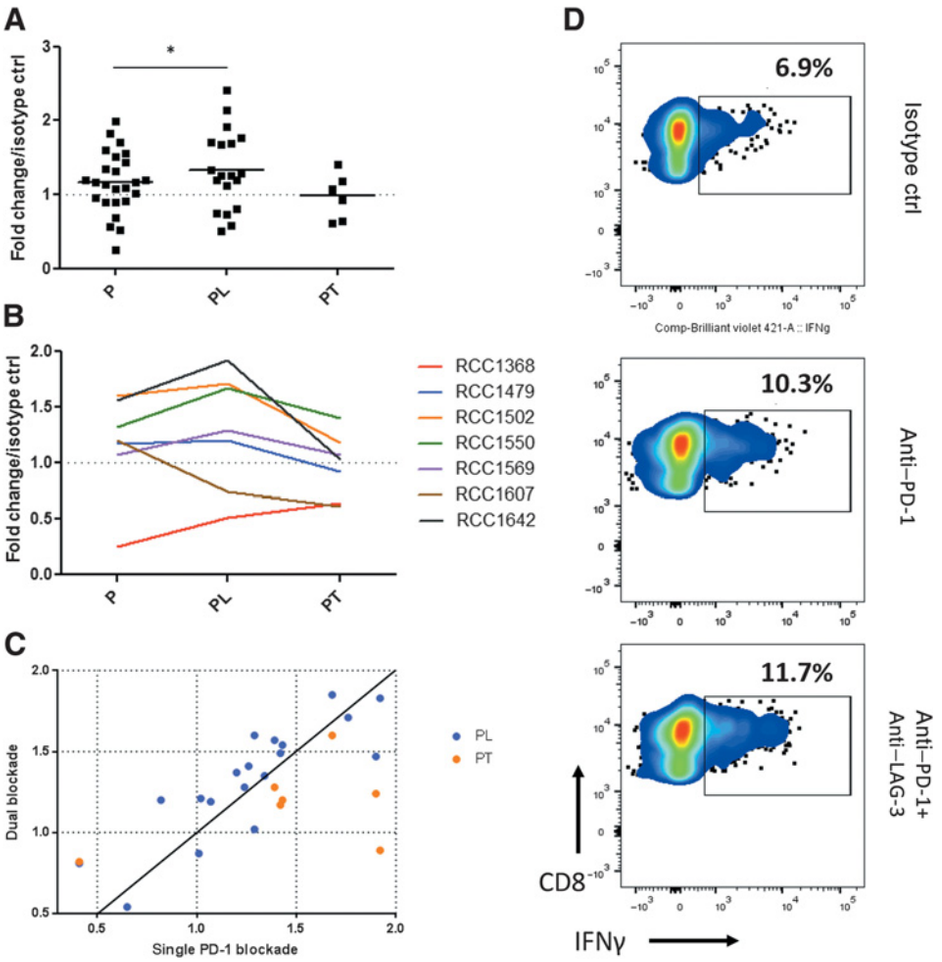

Figure 3.
Functional effects of checkpoint receptor blockade. **A,** Percentages of IFNγ$^+$ CD8$^+$ TILs after a 3-day culture in the presence of anti-CD3. Blocking of inhibitory checkpoint receptors was performed in the presence of P = PD-1, PL = PD-1 + LAG-3, or PT = PD-1 + Tim-3 antagonist Abs. Fold changes as compared with the relevant isotype control Abs (set to 1.0, dotted line) and means are shown (P: $n = 25$; PL: $n = 19$; PT: $n = 7$). Significance was tested with an unpaired t test. *, $P \leq 0.05$. **B,** IFNγ production within CD8$^+$ T cells for the $n = 7$ patients for whom all three experiments were performed. P, PD-1; PL, PD-1 + LAG-3; PT, PD-1 + Tim-3 antagonist Abs. **C,** Mean fold changes obtained in single TIL cultures after single PD-1 blockade (x-axis) versus dual Ab blockade (y-axis; PL = blue, PT = orange). Each point represents 1 patient in one setting. The black line indicates $x = y$. Hence, for all patients above the line, dual blockade led to increased functionality (IFNγ production) as compared with single PD-1 blockade alone. PL, PD-1 + LAG-3; PT, PD-1 + Tim-3 antagonist Abs. **D,** Representative FACS plots for 1 patient (RCC1642). Production of IFNγ within CD8$^+$ cells is shown after 3 days of culture.

phase, the frequency of IFNγ$^+$ (proinflammatory cytokine), CD107a$^+$ (degranulation), and Ki67$^+$ (proliferation) cells was determined within CD8$^+$ and total CD4$^+$ T cells. We then calculated for each functional marker and in each T-cell subset the ratio between the frequencies of marker$^+$ cells obtained in the various blockade settings and the frequencies obtained in the stimulation without iR blockade. Figure 3A shows these ratios for IFNγ production within CD8$^+$ T cells. Blockade of PD-1 alone (P) had only a marginal enhancing effect on CD8$^+$ T-cell function, with a mean fold change of 1.2 (range, 0.3–2.0) as compared with stimulation without iR blockade (Fig. 3A). Blockade of PD-1 and Tim-3 together (PT) did not affect the mean cytokine production (mean fold change of 1.0; range, 0.6–1.4); in contrast, blockade of PD-1 plus LAG-3 (PL) resulted in a statistically significant higher percentage of CD8$^+$ IFNγ$^+$ T cells (mean fold change 1.3; range, 0.5–2.4) compared with stimulation without iR blockade ($P = 0.0176$; Fig. 3A). In 5 of the 7 patients for whom data were available for all three blockade scenarios, we observed an increase of IFNγ$^+$ CD8$^+$ T cells in PL compared with P (Fig. 3B).

On average, functional enhancement after iR blockade was modest for IFNγ, whereas we did not observe any significant differences for CD107a and Ki67 (Supplementary Fig. S4). However, to estimate the overall functionality (proliferation, degranulation, and cytokine production together), we calculated the mean fold change derived from all three functional parameters for each experiment and compared this mean fold change for single PD-1 blockade to blockade of PL or PT (Fig. 3C). When LAG-3 was additionally blocked, immune function was improved in 12 of 19 patients (63%; Fig. 3C). For Tim-3 coblockade, this enhancement was seen in only 1 of 7 patients (14%), indicating that dual PD-1 + LAG-3, but not PD-1 + Tim-3 blockade, is improving immune functions of stimulated RCC TILs ($P = 0.0302$, Fisher exact test; Fig. 3C).

LAG-3 cell-surface expression was upregulated upon PD-1 blockade

Finally, the expression of the receptors PD-1, LAG-3, and Tim-3 was assessed individually in a subgroup of patient samples after the 3-day culture step described above. The frequency of cells expressing each of the three iR was determined within total CD4$^+$ and CD8$^+$ T cells and compared between T cells cultured in the presence of the anti–PD-1 or of an isotype control antibody (Fig. 4). The expression of PD-1 was not affected (mean fold changes for total CD4$^+$ cells: 1.0 ± 0.2; for CD8$^+$ cells: 1.0 ± 0.2) by PD-1 blockade, suggesting that the receptor is not modulated after targeting with antagonistic (therapeutic) Ab (Fig. 4). In contrast, we observed a clear upregulation of LAG-3 after PD-1 blockade on total CD4$^+$ T cells (mean fold change: 1.5 ± 0.6) and on CD8$^+$ T cells (1.3 ± 0.4; Fig. 4). In some donors, LAG-3 expression was increased more than 2-fold. In contrast, Tim-3

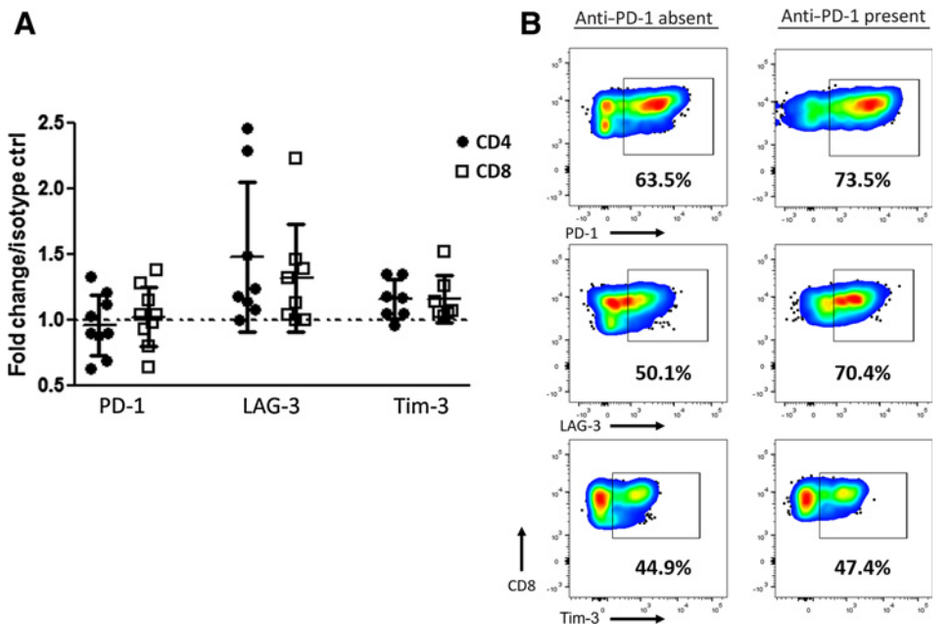

Figure 4.
Expression of checkpoint receptors after *in vitro* PD-1 blockade. **A,** Frequency of PD-1$^+$, LAG-3$^+$, and TIM-3$^+$ cells in total CD4$^+$ (●) and CD8$^+$ (□) T cells after a 3-day culture in the presence of anti-CD3. Fold changes in the percentage of expression of the three iR in the presence of anti–PD-1 relative to isotype control are shown (PD-1 expression was tested in 9 patients, and LAG-3 and Tim-3 in 8 and 7 patients, respectively). Dotted line represents no change (fold change = 1.0). Means and SDs are shown. Significance was tested with a paired *t* test. **B,** Representative FACS plots for 1 patient (RCC1644). CD8 (*y*-axis) versus iR expression (*x*-axis) after 3 days of culture in the presence (right) or absence (left) of anti–PD-1 is shown.

expression appeared less affected by PD-1 blockade (mean fold change: 1.2 ± 0.2 and 1.2 ± 0.2 for both total CD4$^+$ T cells and CD8$^+$ T cells; Fig. 4). Based on these functional experiments, we propose that clinical targeting of PD-1 together with LAG-3 might show synergistic effects and increase clinical response rates in RCC patients.

Discussion

Blockade of immune-checkpoint molecules by antagonist antibodies against CTLA-4 or PD-1/PD-L1 is a game-changing discovery in cancer therapy, also for advanced RCC. However, most RCC patients still do not benefit from this treatment option. Inflamed (also referred to as "hot") tumors that are infiltrated by T cells could benefit from additional measures to counterattack local immunosuppression, such as combinations of checkpoint blockade with chemotherapy—to modulate immunosuppressive cells—or of several checkpoint modulators (28). Hence, targeting multiple inhibitory molecules at once is a current focus of investigation.

In our study, we aimed to identify the most promising inhibitory receptor candidates for a combined immune-checkpoint therapy with anti–PD-1 for advanced RCC patients. By investigating the expression of 5 prominent candidate iR on the surface of human RCC TILs, we observed that PD-1 is the most expressed iR inside the tumor. The next most expressed iR were BTLA and LAG-3, whereas Tim-3 expression was slightly lower. BTLA expression was even higher in PBMCs than in TILs, indicating that this receptor might not be preferentially involved in local intratumor immune suppression. In line with our data, Giraldo and colleagues (looking at a distinct but overlapping panel of T-cell checkpoint receptors) also identify PD-1 and LAG-3 as the most frequently expressed iR in RCC TILs analyzed *ex vivo* (27), whereas expression of all three iR (PD-1, LAG-3, and Tim-3) dominates on RCC TILs after *in vitro* expansion for adoptive cell transfer purposes (29).

We detected CTLA-4 expression (extracellular staining) on only a small fraction of TILs. In a previous phase II trial administering the CTLA-4 antibody ipilimumab, only 6 of 61 mRCC patients experience a partial response (30), and ipilimumab monotherapy has not been tested in phase III studies since then. Remelimumab, another CTLA-4 antibody, was administered together with sunitinib, and although 9 of 21 patients (43%) achieved a partial response, the trial was stopped due to toxicities including unexpected acute renal failure and one sudden death (31). Nevertheless, the combination nivolumab + ipilimumab clearly leads to increased ORR (42% vs. 25%) and OS (not reached vs. 25 months) as compared with nivolumab treatment alone (Checkmate 025 and Checkmate 214 trials; refs. 7, 8). Hence, coblockade of inhibitory T-cell receptors might further increase ORR and OS. Based on our data, we concluded that considered separately, but also taking into account the coexpression profile of the iR on single cells, PD-1 and LAG-3 were the most interesting candidates for dual blockade therapy in RCC.

We analyzed if, and which, functional parameters could be boosted by iR blockade and which blockade strategy led to increased immune function of CD4$^+$ and CD8$^+$ T cells. Overall, the functional alterations that we measured after iR blockade were modest. Other studies came to similar results after *in vitro* iR blockade. For example, Fourcade and colleagues detect 1.2-fold more NY-ESO-1–specific CD8$^+$ T cells in melanoma patients, when cells are expanded *in vitro* in the presence of PD-1 antibody compared with cells supplemented with the relevant isotype control antibodies (32). In a different approach, Wong and colleagues detect an approximately 2.6-fold increase of IFNγ production in MART-$1_{26–35(27L)}$–specific T cells incubated for 11 days in the presence of PD-1 antibodies (22). In our experimental setting, which was designed to be as close as possible to the *in vivo* situation, fresh TIL suspensions were not manipulated and contained T cells, but also tumor cells, as well as other immune cells present in the tumor microenvironment including suppressive subsets (e.g., Tregs).

Despite these overall limited *in vitro* effects in terms of proliferation, cytokine production, and degranulation when adding checkpoint antibodies to the TIL cultures, we observed that the blockade of LAG-3 together with PD-1 led to increased $CD8^+$ T-cell functionality (IFNγ production) as compared with the single PD-1 blockade or the blockade of Tim-3 together with PD-1. Assessing degranulation and proliferation did not reveal any differences between the various blockade scenarios. Because T-cell polyfunctionality has been associated with immune protection (against pathogens), it would be interesting to assess whether additional proinflammatory cytokines are differentially produced after single or dual checkpoint blockade *in vitro*. At least in a murine CLL model, dual PD-1 and LAG-3 checkpoint blockade, not single PD-1, LAG-3 or KLRG1 blockade, limits tumor development, suggesting enhanced antitumor function when two receptors are inhibited (33).

To date, it is unknown if a single T cell expressing other iR in addition to PD-1 is fully released from inhibition when only PD-1 is blocked. Multiparametric flow cytometry allowed us to analyze the iR coexpression on a single-cell level. The single expression of PD-1 was the most frequent observed iR^+ profile. Giraldo and colleagues observe that among $CD8^+$ $PD\text{-}1^+$ RCC TILs, iR expression (here Tim-3 and LAG-3 analyzed separately) is only prominent in one subset of patients, predefined by hierarchical unsupervised clustering. This cluster is characterized by reduced disease-free survival (27). Although the coexpression of at least two iR was rather infrequent in our data set, PD-1 and LAG-3 coexpression was clearly the most common event, followed by PD-1 and Tim-3 combination. Hence, blockade of LAG-3, rather than Tim-3, together with PD-1 might be the more reasonable treatment option for RCC, assuming that there are no major functional differences between the two iR. Finally, it is important to note that, in contrast to the general notion of a massive exhaustion inside the tumor, the most frequent population of infiltrated lymphocytes expressed none of the five investigated iR.

We have additionally investigated functional and phenotypic alterations after PD-1 blockade in a short-term *in vitro* assay. TILs were cultured for 3 days in the presence of CD3 antibody and one or more iR antibodies. We observed that the increase in the frequency of $LAG\text{-}3^+$ cells was more prominent than that of $Tim\text{-}3^+$ cells after PD-1 blockade. Upregulation of Tim-3 on T cells has been observed after PD-1 blockade in 2 patients with lung carcinoma (34), and also *in vitro* on TILs obtained from head and neck carcinoma patients (35). Hence, it might well be that blocking PD-1 signaling leads to upregulation of further iR, and that these iR could be different depending on the tumor type, or even on the patient's "immune susceptibility." Whether *in vitro* testing might help to predict long-term *in vivo* impact of PD-1 therapy needs to be more systematically explored.

Clustering of patients according to the expression of surface markers revealed a group of patients predominantly characterized by high frequencies of $LAG\text{-}3^+$ cells with more advanced disease stages (5 from 7 patients diagnosed with metastatic disease, and 5 from 6 patients with relapse during follow-up had primary tumors with marked LAG-3 expression). LAG-3 has been shown to be linked to survival of advanced RCC patients multiple times (16, 27, 36).

Although Tim-3 expression affects the survival of advanced RCC patients (17), both our phenotypic and functional analyses suggest that LAG-3 was a more promising target for a combined blockade therapy with PD-1 in RCC. Whether the blockade of an additional iR studied would further improve checkpoint blockade is disputable, as cells expressing more than two iR were even more infrequent, especially on $CD4^+$ T cells. Furthermore, adverse side effects might increase with every further administered antibody.

In summary, these observations indicated that the blockade of LAG-3, rather than Tim-3, together with PD-1 might be a viable treatment option in advanced RCC, because more T cells will be targeted, namely, single $PD\text{-}1^+$ cells, single $LAG\text{-}3^+$ cells, and those which (neo)express both iR simultaneously. Notably, our samples were all obtained from primary RCC tumors, and it remains to be determined whether (co)expression of iR on infiltrating T cells is similar in primary versus metastatic tissues. At least PD-1 and LAG-3 were found to be similarly expressed in primary ccRCC versus lung metastases in a large patient cohort (22). iR expression might, however, vary depending on the metastatic site (16). Another limitation of our study, especially regarding functional assessments, was the limited amount of tumor-infiltrating cells that can be recovered from the tumor fragments, which hindered the testing of multiple combinations of antibodies for all patients. Finally, it remains to be tested whether these results can be translated to the clinic. Such data are missing so far, but clinical trials targeting Tim-3 or LAG-3 alone or in combination with PD-1 (e.g., NCT02608268, NCT02460224, NCT03005782, and NCT02658981) are currently ongoing in advanced RCC. Once confirmed, our model, which is based on human *ex vivo* and *in vitro* data only, could be expanded to other inhibitory (e.g., TIGIT) and activating candidate molecules (e.g., OX-40), and tested for further cancer entities. In addition to established predictive biomarkers such as PD-L1 intratumoral expression and possibly mutation load, phenotypic analysis of individual patient's TILs for (co)expression of checkpoint receptors together with *in vitro* short-term experiments might help to personalize checkpoint combination therapy and ultimately increase clinical response rate.

Disclosure of Potential Conflicts of Interest

J. Bedke is a consultant for Astellas, AstraZeneca, Bristol-Myers Squibb, Eisai, EUSA, Ipsen, MSD, Novartis, Roche, and Pfizer, reports receiving a commercial research grant from Boehringer, reports receiving other commercial research support from Bristol-Myers Squibb, Eisai, Ipsen, MSD, Novartis, Roche, and Pfizer, and reports receiving speakers bureau honoraria from Bristol-Myers Squibb, Eisai, Ipsen, MSD, Novartis, Roche, EUSA, and Pfizer. H.-G. Rammensee reports receiving a commercial research grant from Boehringer Ingelheim and has ownership interest (including patents) in CureVac. C. Gouttefangeas reports receiving a commercial research grant from Boehringer Ingelheim RCV. No potential conflicts of interest were disclosed by the other authors.

Authors' Contributions

Conception and design: H. Zelba, J. Bedke, M. Zettl, C. Gouttefangeas
Development of methodology: H. Zelba
Acquisition of data (provided animals, acquired and managed patients, provided facilities, etc.): H. Zelba, J. Bedke, J. Hennenlotter
Analysis and interpretation of data (e.g., statistical analysis, biostatistics, computational analysis): H. Zelba, M. Zettl, T. Zichner, A. Chandran, A. Stenzl, C. Gouttefangeas
Writing, review, and/or revision of the manuscript: H. Zelba, J. Bedke, J. Hennenlotter, S. Mostböck, M. Zettl, T. Zichner, A. Chandran, A. Stenzl, H.-G. Rammensee, C. Gouttefangeas
Administrative, technical, or material support (i.e., reporting or organizing data, constructing databases): H. Zelba, J. Hennenlotter, S. Mostböck
Study supervision: J. Bedke, M. Zettl, A. Stenzl, H.-G. Rammensee, C. Gouttefangeas

Acknowledgments

This work was supported by a grant from Boehringer Ingelheim RCV. The authors thank Ursula Kühs, Jana Rokitzki, and Johanna Bödder for technical support and patient follow-up.

The costs of publication of this article were defrayed in part by the payment of page charges. This article must therefore be hereby marked *advertisement* in accordance with 18 U.S.C. Section 1734 solely to indicate this fact.

Received February 25, 2019; revised May 23, 2019; accepted August 30, 2019; published first September 4, 2019.

References

1. Ljungberg B, Bensalah K, Canfield S, Dabestani S, Hofmann F, Hora M, et al. EAU guidelines on renal cell carcinoma: 2014 update. Eur Urol 2015; 67:913–24.
2. Ferlay J, Steliarova-Foucher E, Lortet-Tieulent J, Rosso S, Coebergh JW, Comber H, et al. Cancer incidence and mortality patterns in Europe: estimates for 40 countries in 2012. Eur J Cancer 2013;49:1374–403.
3. Gill DM, Hahn AW, Hale P, Maughan BL. Overview of current and future first-line systemic therapy for metastatic clear cell renal cell carcinoma. Curr Treat Options Oncol 2018;19:6.
4. Bedke J, Gauler T, Grunwald V, Hegele A, Herrmann E, Hinz S, et al. Systemic therapy in metastatic renal cell carcinoma. World J Urol 2017;35:179–88.
5. Lokich J. Spontaneous regression of metastatic renal cancer. Case report and literature review. Am J Clin Oncol 1997;20:416–8.
6. Bedke J, Stuhler V, Stenzl A, Brehmer B. Immunotherapy for kidney cancer: status quo and the future. Curr Opin Urol 2018;28:8–14.
7. Motzer RJ, Escudier B, McDermott DF, George S, Hammers HJ, Srinivas S, et al. Nivolumab versus everolimus in advanced renal-cell carcinoma. N Engl J Med 2015;373:1803–13.
8. Motzer RJ, Tannir NM, McDermott DF, Aren Frontera O, Melichar B, Choueiri TK, et al. Nivolumab plus ipilimumab versus sunitinib in advanced renal-cell carcinoma. N Engl J Med 2018;378:1277–90.
9. Sharma P, Allison JP. The future of immune checkpoint therapy. Science 2015;348:56–61.
10. Taube JM, Klein A, Brahmer JR, Xu H, Pan X, Kim JH, et al. Association of PD-1, PD-1 ligands, and other features of the tumor immune microenvironment with response to anti-PD-1 therapy. Clin Cancer Res 2014;20: 5064–74.
11. Lipson EJ, Forde PM, Hammers HJ, Emens LA, Taube JM, Topalian SL. Antagonists of PD-1 and PD-L1 in cancer treatment. Semin Oncol 2015;42: 587–600.
12. Rizvi NA, Hellmann MD, Snyder A, Kvistborg P, Makarov V, Havel JJ, et al. Cancer immunology. Mutational landscape determines sensitivity to PD-1 blockade in non-small cell lung cancer. Science 2015;348:124–8.
13. Teng MW, Ngiow SF, Ribas A, Smyth MJ. Classifying cancers based on T-cell infiltration and PD-L1. Cancer Res 2015;75:2139–45.
14. Anderson AC, Joller N, Kuchroo VK. Lag-3, Tim-3, and TIGIT: co-inhibitory receptors with specialized functions in immune regulation. Immunity 2016;44:989–1004.
15. Pardoll DM. The blockade of immune checkpoints in cancer immunotherapy. Nat Rev Cancer 2012;12:252–64.
16. Giraldo NA, Becht E, Pages F, Skliris G, Verkarre V, Vano Y, et al. Orchestration and prognostic significance of immune checkpoints in the microenvironment of primary and metastatic renal cell cancer. Clin Cancer Res 2015;21:3031–40.
17. Granier C, Dariane C, Combe P, Verkarre V, Urien S, Badoual C, et al. Tim-3 expression on tumor-infiltrating PD-1(+)CD8(+) T cells correlates with poor clinical outcome in renal cell carcinoma. Cancer Res 2017;77:1075–82.
18. Chandran PA, Laske K, Cazaly A, Rusch E, Schmid-Horch B, Rammensee HG, et al. Validation of immunomonitoring methods for application in clinical studies: The HLA-peptide multimer staining assay. Cytometry B Clin Cytom 2018;94:342–53.
19. Laske K, Shebzukhov YV, Grosse-Hovest L, Kuprash DV, Khlgatian SV, Koroleva EP, et al. Alternative variants of human HYDIN are novel cancer-associated antigens recognized by adaptive immunity. Cancer Immunol Res 2013;1:190–200.
20. Stecher C, Battin C, Leitner J, Zettl M, Grabmeier-Pfistershammer K, Holler C, et al. PD-1 blockade promotes emerging checkpoint inhibitors in enhancing T cell responses to allogeneic dendritic cells. Front Immunol 2017;8:572.
21. Fourcade J, Sun Z, Pagliano O, Guillaume P, Luescher IF, Sander C, et al. CD8(+) T cells specific for tumor antigens can be rendered dysfunctional by the tumor microenvironment through upregulation of the inhibitory receptors BTLA and PD-1. Cancer Res 2012;72:887–96.
22. Wong RM, Scotland RR, Lau RL, Wang C, Korman AJ, Kast WM, et al. Programmed death-1 blockade enhances expansion and functional capacity of human melanoma antigen-specific CTLs. Int Immunol 2007;19: 1223–34.
23. Patnaik A, Kang SP, Rasco D, Papadopoulos KP, Elassaiss-Schaap J, Beeram M, et al. Phase I study of pembrolizumab (MK-3475; anti-PD-1 monoclonal antibody) in patients with advanced solid tumors. Clin Cancer Res 2015;21:4286–93.
24. Pluim D, Ros W, van Bussel MTJ, Brandsma D, Beijnen JH, Schellens JHM. Enzyme linked immunosorbent assay for the quantification of nivolumab and pembrolizumab in human serum and cerebrospinal fluid. J Pharm Biomed Anal 2019;164:128–34.
25. Attig S, Hennenlotter J, Pawelec G, Klein G, Koch SD, Pircher H, et al. Simultaneous infiltration of polyfunctional effector and suppressor T cells into renal cell carcinomas. Cancer Res 2009;69:8412–9.
26. Martens A, Wistuba-Hamprecht K, Geukes Foppen M, Yuan J, Postow MA, Wong P, et al. Baseline peripheral blood biomarkers associated with clinical outcome of advanced melanoma patients treated with ipilimumab. Clin Cancer Res 2016;22:2908–18.
27. Giraldo NA, Becht E, Vano Y, Petitprez F, Lacroix L, Validire P, et al. Tumor-infiltrating and peripheral blood T-cell immunophenotypes predict early relapse in localized clear cell renal cell carcinoma. Clin Cancer Res 2017;23: 4416–28.
28. Palucka AK, Coussens LM. The basis of oncoimmunology. Cell 2016;164: 1233–47.
29. Andersen R, Westergaard MCW, Kjeldsen JW, Muller A, Pedersen NW, Hadrup SR, et al. T-cell responses in the microenvironment of primary renal cell carcinoma-implications for adoptive cell therapy. Cancer Immunol Res 2018;6:222–35.
30. Yang JC, Hughes M, Kammula U, Royal R, Sherry RM, Topalian SL, et al. Ipilimumab (anti-CTLA4 antibody) causes regression of metastatic renal cell cancer associated with enteritis and hypophysitis. J Immunother 2007; 30:825–30.
31. Rini BI, Stein M, Shannon P, Eddy S, Tyler A, Stephenson JJ Jr., et al. Phase 1 dose-escalation trial of tremelimumab plus sunitinib in patients with metastatic renal cell carcinoma. Cancer 2011;117:758–67.
32. Fourcade J, Sun Z, Pagliano O, Chauvin JM, Sander C, Janjic B, et al. PD-1 and Tim-3 regulate the expansion of tumor antigen-specific CD8(+) T cells induced by melanoma vaccines. Cancer Res 2014;74:1045–55.
33. Wierz M, Pierson S, Guyonnet L, Viry E, Lequeux A, Oudin A, et al. Dual PD1/LAG3 immune checkpoint blockade limits tumor development in a murine model of chronic lymphocytic leukemia. Blood 2018;131: 1617–21.
34. Koyama S, Akbay EA, Li YY, Herter-Sprie GS, Buczkowski KA, Richards WG, et al. Adaptive resistance to therapeutic PD-1 blockade is associated with upregulation of alternative immune checkpoints. Nat Commun 2016;7: 10501.
35. Shayan G, Srivastava R, Li J, Schmitt N, Kane LP, Ferris RL. Adaptive resistance to anti-PD1 therapy by Tim-3 upregulation is mediated by the PI3K-Akt pathway in head and neck cancer. Oncoimmunology 2017;6: e1261779.
36. Becht E, Giraldo NA, Beuselinck B, Job S, Marisa L, Vano Y, et al. Prognostic and theranostic impact of molecular subtypes and immune classifications in renal cell cancer (RCC) and colorectal cancer (CRC). Oncoimmunology 2015;4:e1049804.